AN EXPERIMENTAL STUDY OF VLF MODE COUPLING AND POLARIZATION REVERSAL*

by

Paul Rodriguez
and
Donald A. Gurnett

This work was supported in part by the Office of Naval Research under Contract No. N00014-68-A-0196-0003

Department of Physics and Astronomy
THE UNIVERSITY OF IOWA
Iowa City, Iowa

U of Iowa 70-23

AN EXPERIMENTAL STUDY OF VLF MODE COUPLING AND POLARIZATION REVERSAL*

by

Paul Rodriguez
and
Donald A. Gurnett

March 1970

Department of Physics and Astronomy
The University of Iowa
Iowa City, Iowa

*Research supported in part by the National Aeronautics and Space Administration under Contracts NAS5-10625, NAS1-8141, NAS1-8144, NAS1-8150, and NGR-16-001-043; and by the Office of Naval Research under Contract N00014-68-A-0196-0003.

UNCLASSIFIED

Security Classification

DOCUMENT CONTROL DATA - R&D

(Security classification of title, body of abstract and indexing annotation must be entered when the overall report is classified)

1. ORIGINATING ACTIVITY *(Corporate author)*
The University of Iowa
Department of Physics and Astronomy

2a. REPORT SECURITY CLASSIFICATION
UNCLASSIFIED

2b GROUP
VLF

3. REPORT TITLE
An Experimental Study of VLF Mode Coupling and Polarization Reversal

4. DESCRIPTIVE NOTES *(Type of report and inclusive dates)*
Progress March 1970

5. AUTHOR(S) *(Last name, first name, initial)*
Rodriguez, P. and Gurnett, D. A.

6. REPORT DATE	7a. TOTAL NO. OF PAGES	7b. NO. OF REFS
March 1970	36	16

8a. CONTRACT OR GRANT NO.
N00014-68-A-0196-0003

b. PROJECT NO.

c.

d.

9a. ORIGINATOR'S REPORT NUMBER(S)
U. of Iowa 70-23

9b. OTHER REPORT NO(S) *(Any other numbers that may be assigned this report)*

10. AVAILABILITY/LIMITATION NOTICES
Distribution of this document is unlimited

11. SUPPLEMENTARY NOTES

12. SPONSORING MILITARY ACTIVITY
Office of Naval Research

13. ABSTRACT

[SEE FOLLOWING PAGE]

DD FORM 1 JAN 64 1473

UNCLASSIFIED

Security Classification

14. KEY WORDS	LINK A		LINK B		LINK C	
	ROLE	WT	ROLE	WT	ROLE	WT
Ion Cyclotron Whistlers						
Polarization Reversal						
Mode Coupling						

INSTRUCTIONS

1. ORIGINATING ACTIVITY: Enter the name and address of the contractor, subcontractor, grantee, Department of Defense activity or other organization *(corporate author)* issuing the report.

2a. REPORT SECURITY CLASSIFICATION: Enter the overall security classification of the report. Indicate whether "Restricted Data" is included. Marking is to be in accordance with appropriate security regulations.

2b. GROUP: Automatic downgrading is specified in DoD Directive 5200.10 and Armed Forces Industrial Manual. Enter the group number. Also, when applicable, show that optional markings have been used for Group 3 and Group 4 as authorized.

3. REPORT TITLE: Enter the complete report title in all capital letters. Titles in all cases should be unclassified. If a meaningful title cannot be selected without classification, show title classification in all capitals in parenthesis immediately following the title.

4. DESCRIPTIVE NOTES: If appropriate, enter the type of report, e.g., interim, progress, summary, annual, or final. Give the inclusive dates when a specific reporting period is covered.

5. AUTHOR(S): Enter the name(s) of author(s) as shown on or in the report. Enter last name, first name, middle initial. If military, show rank and branch of service. The name of the principal author is an absolute minimum requirement.

6. REPORT DATE: Enter the date of the report as day, month, year; or month, year. If more than one date appears on the report, use date of publication.

7a. TOTAL NUMBER OF PAGES: The total page count should follow normal pagination procedures, i.e., enter the number of pages containing information.

7b. NUMBER OF REFERENCES: Enter the total number of references cited in the report.

8a. CONTRACT OR GRANT NUMBER: If appropriate, enter the applicable number of the contract or grant under which the report was written.

8b, 8c, & 8d. PROJECT NUMBER: Enter the appropriate military department identification, such as project number, subproject number, system numbers, task number, etc.

9a. ORIGINATOR'S REPORT NUMBER(S): Enter the official report number by which the document will be identified and controlled by the originating activity. This number must be unique to this report.

9b. OTHER REPORT NUMBER(S): If the report has been assigned any other report numbers *(either by the originator or by the sponsor)*, also enter this number(s).

10. AVAILABILITY/LIMITATION NOTICES: Enter any limitations on further dissemination of the report, other than those imposed by security classification, using standard statements such as:

(1) "Qualified requesters may obtain copies of this report from DDC."

(2) "Foreign announcement and dissemination of this report by DDC is not authorized."

(3) "U. S. Government agencies may obtain copies of this report directly from DDC. Other qualified DDC users shall request through _____."

(4) "U. S. military agencies may obtain copies of this report directly from DDC. Other qualified users shall request through _____."

(5) "All distribution of this report is controlled. Qualified DDC users shall request through _____."

If the report has been furnished to the Office of Technical Services, Department of Commerce, for sale to the public, indicate this fact and enter the price, if known.

11. SUPPLEMENTARY NOTES: Use for additional explanatory notes.

12. SPONSORING MILITARY ACTIVITY: Enter the name of the departmental project office or laboratory sponsoring *(paying for)* the research and development. Include address.

13. ABSTRACT: Enter an abstract giving a brief and factual summary of the document indicative of the report, even though it may also appear elsewhere in the body of the technical report. If additional space is required, a continuation sheet shall be attached.

It is highly desirable that the abstract of classified reports be unclassified. Each paragraph of the abstract shall end with an indication of the military security classification of the information in the paragraph, represented as *(TS)*, *(S)*, *(C)*, or *(U)*.

There is no limitation on the length of the abstract. However, the suggested length is from 150 to 225 words.

14. KEY WORDS: Key words are technically meaningful terms or short phrases that characterize a report and may be used as index entries for cataloging the report. Key words must be selected so that no security classification is required. Identifiers, such as equipment model designation, trade name, military project code name, geographic location, may be used as key words but will be followed by an indication of technical context. The assignment of links, roles, and weights is optional.

ABSTRACT

Below the proton gyrofrequency, both polarization reversal and mode coupling of the right and left hand modes of propagation can occur. In this paper an experimental study of polarization reversal and mode coupling of electron and proton whistlers is presented. The occurrence of polarization reversal for a whistler signal observed in the ionosphere is indicated by the presence of a proton whistler. Mode coupling between the right and left hand modes of propagation is indicated by the occurrence of both electron and proton whistler signals at the same frequency.

Mode coupling is observed to occur most frequently over a range of about 35° - 55° magnetic latitude. Below about 35° magnetic latitude, polarization reversal is the predominant effect, whereas above about 55° magnetic latitude neither mode coupling nor polarization reversal occur and proton whistlers are not observed. These results are compared with existing theories to explain this latitude dependence.

I. INTRODUCTION

Polarization reversal and mode coupling of electromagnetic waves in the ionosphere has been discussed by Gurnett, Shawhan, Brice and Smith [1965] (hereafter referred to as GSBS) and by Jones [1968, 1969] in connection with ion cyclotron whistlers observed by satellites [Smith, et al., 1964]. GSBS considered a collisionless model of the ionosphere in explaining the polarization reversal of ion cyclotron whistlers and showed that mode coupling must be included in order to explain the observed transmission of both electron and proton whistlers signals from the ground to the satellite at frequencies below the proton gyrofrequency. They describe mode coupling in terms of a critical angle θ_c, where θ is the angle between the geomagnetic field $\vec{B}_o$ and the wave normal direction $\vec{K}$. An upgoing electron whistler propagating near the cone of angles defined by θ_c results in both electron and ion whistlers being present above the "cross-over" altitude, the altitude at which the refractive indices of the two modes are equal. For the model used by GSBS, θ_c is of the order of 10°.

Jones [1968, 1969] has further extended the work of GSBS by showing in detail how the wave polarization varies

near the crossover altitude, and how the wave normal angle and the critical coupling angle control polarization reversal and mode coupling phenomena. Using the ion density profile of GSBS and a realistic model of collision frequencies vs. altitude, Jones has computed values of θ_c at the crossover altitude as a function of frequency and latitude. His calculations predicted a marked dependence of mode coupling and polarization reversal on latitude. It is the purpose of this paper to report on an experimental investigation of mode coupling and polarization reversal of electron and proton whistlers and compare these results with Jones' predictions.

II. POLARIZATION REVERSAL AND MODE COUPLING

Mode coupling of ion cyclotron whistlers in the ionosphere can be described using Forsterling's coupled equations for vertical incidence in an inhomogeneous, anisotropic medium [Budden, 1961]:

$$\begin{aligned} F_o'' + F_o(n_o^2 + \psi^2) &= \psi' F_x + 2\psi F_x' \\ F_x'' + F_x(n_x^2 + \psi^2) &= \psi' F_o + 2\psi F_o' \end{aligned} \tag{1}$$

where F_o and F_x are proportional to the fields in the ordinary and extraordinary modes, respectively. The prime denotes $1/K\ \partial/\partial z$, where $K = n\omega/c$ is the wave number and z is the vertical coordinate. n_o and n_x are the indices of refraction for the respective modes, and ψ is the "coupling parameter," so called because when $\psi = 0$ the equations are independent and the two modes propagate independently, while if $\psi \neq 0$, the equations are coupled and there is interaction between the modes. ψ has the form

$$\psi = \frac{\rho_o'}{(\rho_o^2 - 1)} = \frac{\rho_x'}{(\rho_x^2 - 1)} \tag{2}$$

where ρ is the polarization, E_y/E_x, defined in terms of the components of the electric field which lie in the wavefront.

π_k = plasma frequency of the kth species, and

Ω_k = gyrofrequency of the kth species.

For propagation parallel to the static magnetic field, R and L are the indices of refraction squared for the right and left hand circularly polarized modes, respectively. In a collisionless plasma, R and L are real quantities so that ρ is imaginary. The critical coupling condition $\rho = \pm 1$, therefore cannot be satisfied, except for the singular case of propagation exactly along the geomagnetic field, $\theta = 0$. In order for the critical coupling condition to be satisfied at an angle other than $\theta = 0$, GSBS concluded that collisions must be considered in order that ρ have a real part to satisfy the critical coupling condition.

Collisions may be included by replacing the mass m_k in R, L, and P with $m_k(1 + \frac{i\nu_k}{\omega})$, where ν_k is the collision frequency of the kth species. The equations R, L, S, D, and P then become complex ($R = R_r + iR_i$, ...). For small collision frequencies and to a first order approximation, the real parts of these equations remain the same as in the collisionless case and the imaginary parts are small compared to the real part except near the poles or zeros

of these functions. When R is approximately equal to L (D = 0), which will be of primary interest for proton whistler mode coupling, equation (3) may be written approximately

$$\rho = \frac{i(D_r + iD_i)n^2 \cos \theta}{Sn^2 - RL} , \qquad (4)$$

where the imaginary parts of R, L and S are neglected since they are small compared to the real part. From equation (4) it is seen that the critical coupling condition $\rho = \pm 1$, requires that the following two conditions be satisfied simultaneously (from the real and imaginary parts of ρ):

$$D_r = 0 \qquad (5)$$

$$\frac{D_i n^2 \cos \theta}{Sn^2 - RL} = \pm 1 \qquad (6)$$

The first condition $D_r = 1/2(R - L) = 0$ requires that the real parts of the refractive indices for the right and left hand modes be equal (R = L). This condition is called the crossover condition, and the corresponding frequency is called the crossover frequency [Smith and Brice, 1964].

The second condition, equation (6), determines the wave normal angle θ_c, called the critical coupling angle, at which critical coupling occurs. Two waves propagating in the right and left hand modes with wave normal angles near θ_c will be strongly coupled at the altitude where the wave frequency equals the crossover frequency.

Figure 1 shows the crossover frequency ($D = 0$), the proton gyrofrequency ($L = \infty$), and various other characteristic frequencies as a function of altitude for the ionospheric model used by GSBS. The cross-hatched region between the crossover frequency and the proton gyrofrequency is where both the right and left hand modes can propagate.

When collisions are included, the polarization can also be expressed by an equation due to Jones [1968],

$$\rho^2 + \frac{2i}{G}\frac{\sin^2\theta}{\cos\theta}\rho + 1 = 0 \qquad (7)$$

where

$$G = \frac{P(L - R)}{RL - PS}$$

The roots of equation (7) are the polarization of the R and L modes. The significance of the critical coupling angle can be displayed graphically by plotting the roots of equation (7) on the complex polarization plane as a

function of altitude near the crossover altitude. Figure 2 is taken from Jones [1968] and shows such a plot for various wave normal angles using the ionospheric model of Figure 1 and a wave frequency of 400 Hz. The upper half of the complex ρ plane in Figure 2 is for the left hand polarized mode and the lower half plane is for the right hand polarized mode. (Jones uses the definitions $\rho = -i$ for right and $\rho = +i$ for left hand polarization.) The critical coupling angle for the conditions at the crossover altitude (772 km) is $\theta_c = 8.9°$. From Figure 2 it is seen that for wave normal angles less than θ_c (for example $\theta = 8°$, labeled A in Figure 2) the polarization paths do not cross the real ρ axis, therefore the sense of polarization, right or left hand, does not change as the wave passes the crossover altitude. For wave normal angles greater than θ_c (for example $\theta = 10°$, labeled E in Figure 2) the polarization path starts at $\rho = -i$ (right hand) and terminates at $\rho = +i$ (left hand), with the polarization reversal occurring as the wave passes the crossover altitude. In both cases illustrated ($\theta = 8°$ and $\theta = 10°$) the polarization does not come close to $\rho = \pm 1$ (the critical coupling condition) so mode coupling is negligible.

For wave normal angles close to $\theta_c = 8.9°$, it can be seen from Figure 2 that the polarization path passes

very close to $\rho = 1$ (inside the dotted circle, for example) and strong coupling will occur as the coupling parameter ψ become large at $\rho = +1$. For wave normal angles close to the critical coupling angle an upward traveling right hand polarized wave below the crossover altitude will be split into right and left hand polarized waves upon passing the crossover altitude.

These conclusions can be summarized as follows:

(a) $\theta > \theta_c$. Polarization reversal and negligible mode coupling. An upward traveling wave in the R mode changes smoothly into an upward traveling wave in the L mode upon passing the crossover altitude. If $|\theta - \theta_c|$ is small, weak coupling may generate a small amount of energy in the R mode above the crossover altitude.

(b) $\theta \simeq \theta_c$. Critical coupling. An upward traveling wave in the R mode is split into two upward traveling waves in the R and L modes as ψ, the coupling parameter, becomes large as the polarization approaches $\rho = \pm 1$. A determination of the splitting of the energy into the two modes requires a full wave solution.

(c) $\theta<\theta_c$. No polarization reversal and negligible mode coupling. An upward traveling wave in the R mode remains in the R mode. If $|\theta - \theta_c|$ is small, weak coupling may generate a small amount of energy in the L mode above the cross-over altitude.

Because of the large refractive index in the ionosphere at VLF frequencies, the wave normal direction of a whistler entering the ionosphere from below will be refracted to nearly vertical upon entering the ionosphere. In the absence of horizontal gradients, the wave normal of the whistler is determined by the dip angle of the geomagnetic field. The polarization reversal and mode coupling processes discussed above are, therefore, expected to be strongly latitude dependent.

Jones [1968, 1969] has considered the latitude dependence of polarization reversal and mode coupling for proton whistlers, and his results are summarized in Figure 3. Jones' classification considered three coupling types: fully formed proton whistlers, partially formed proton whistlers, and no proton whistlers, corresponding respectively to wave normal angles greater than, comparable to, and less than the critical coupling angle. At low latitudes where the geomagnetic field makes a large angle relative to vertical, the wave normal angle

is greater than θ_c so that only fully formed proton whistlers should be observed. At high latitudes where the geomagnetic field is nearly vertical, the wave normal angle is less than θ_c so that polarization reversal does not occur and no proton whistler should be observed. The computed transition latitudes between fully formed, partially formed, and no proton whistler, are given by Jones in Figure 3. The transition latitudes are dependent on altitude because of the altitude dependence of the collision frequencies and other parameters which determine the critical coupling angle.

III. CLASSIFICATION OF COUPLING TYPES

In the present study of mode coupling and polarization reversal, spectrograms of whistlers are classified according to the scheme given in Figure 4. These classifications have been selected after a detailed study of several hundred individual whistler spectrograms to insure that all types of observed mode coupling and polarization reversal phenomena can be included in this classification. In this respect, "partially formed" proton whistlers, as defined by Jones and consisting of proton whistlers with cutoffs at frequencies intermediate between the crossover frequency and the proton gyrofrequency, are rarely observed.

A. Type C_1, Polarization Reversal and No Coupling. In this coupling type, the observed spectrogram shows only a proton whistler between the crossover frequency, ω_{12}, and the proton gyrofrequency, Ω_1. No electron whistler signal is seen in the frequency range from ω_{12} to Ω_c (see Figure 4a).

B. Type C_2, Polarization Reversal and Weak Coupling. In this coupling type, a weak electron whistler is observed in the frequency range from ω_{12} to Ω_c (dashed line in Figure 4b), while most of the signal strength in the fre-

quency range ω_{12} to Ω_1 is in the proton whistler. Thus, weak coupling and polarization reversal has occurred near the crossover altitude.

C. Type C_3, Strong Coupling. In this coupling type, the signal strength of the proton and electron whistlers in the frequency range from ω_{12} to Ω_1 are observed to be approximately the same (see Figure 4c). Thus, strong coupling of the two waves has occurred at the crossover altitude.

D. Type C_4, No Polarization Reversal and Weak Coupling. In this coupling type, a weak proton whistler is observed in the frequency range from ω_{12} to Ω_1, but most of the signal strength remains in the electron whistler (see Figure 4d).

E. Type C_5, No Polarization Reversal and No Coupling. In this coupling type, no proton whistler is observed above the crossover altitude. Neither polarization reversal nor mode coupling occurs. For this case, it is necessary that the electron whistler be observed at frequencies below the proton gyrofrequency so that the absence of a proton whistler can be ascertained. If the electron whistler is not observed at any frequency below the proton gyrofrequency, then the absence of a proton whistler could be due to the absence of low-frequency

components in the original lightning impulse. Cases for which no electron whistler signal was observed below the proton gyrofrequency were excluded from this study.

IV. STATISTICAL SURVEY OF MODE COUPLING

Spectrograms of whistlers for this study were obtained from satellites Injun 3 and Injun 5, both of which are low altitude polar orbiting satellites. These satellites both carried very-low-frequency receivers covering the frequency range from a few tens of Hz to 10KHz. Details of the VLF experiments on these satellites are given in Gurnett and O'Brien [1964] and Gurnett et al. [1969].

During a satellite pass where many whistlers are occurring, a progression of coupling types from C_1 at low geomagnetic latitudes, to C_5 at higher geomagnetic latitudes is generally observed. Figure 5 shows portions of such a pass near the transition latitudes. The magnetic antenna data shows that beginning at a geomagnetic latitude (GML) of 26.7° (The low latitude portion of this pass is not shown in Figure 5.) coupling type C_1 is being observed up to a latitude of about 39°. Between geomagnetic latitudes of 39° and 54°, coupling types C_2, C_3, and C_4 are primarily observed. Above 54°, mostly type C_5 is observed. On this pass, the transition latitudes defined by Jones and shown in Figure 3 are 39° and 54°, respectively. The "smooth" behavior in coupling variation with latitude seen in this pass is not typical, however. Figure 6 shows a portion of a pass in which clear

transition latitudes are not evident. Different coupling types are occurring close together and not in the expected latitudinal sequence. For example, near geomagnetic latitude 50°, types C_1 are observed, while at about 40°, types C_2 and C_4 can be seen. The determination of transition latitudes must therefore be based on the frequencies of occurrence of coupling types C_2, C_3, and C_4. This has been done for the transitions near 37° and 56° GML in Figure 6. Of about 60 summer-night passes studied, there were only about 25% that showed distinct transition latitudes as in Figure 5. Most passes were of the type shown in Figure 6. Most passes also show a latitudinal cutoff of whistler signals in the vicinity of 60° geomagnetic latitude (indicated in Figure 6 at about 57° GML) which has been associated with the position of the plasmapause [Carpenter et al., 1968; Taylor et al., 1969; Heyborne et al., 1969].

In Figure 7, 30 summer-night passes have been plotted. The portion of each pass between the transition latitudes is shown by the solid line. The lines A and A' are the average boundaries marking out the transition region. The portions of each pass shown by the dashed and dotted lines correspond to the occurrence of primarily C_1 and C_5 coupling types, respectively. A latitudinal cutoff in whistler activ-

ity is indicated by a cross on each pass in which it was observed to occur. The transition latitudes computed by Jones are also indicated in Figure 7 for comparison.

In addition to mode coupling, another important feature related to the critical coupling angle θ_c is the electron whistler cutoff frequency Ω_c, indicated in Figure 4. Jones [1969] shows that, when collisions are included, Ω_c is the frequency for which the critical coupling angle θ_c is equal to the wave normal angle θ. Since θ_c depends on magnetic latitude and altitude, Ω_c also varies with magnetic latitude and altitude. In Figure 8, Jones' curve for Ω_c is reproduced as the solid line. Beside each point is written the altitude above which the corresponding value of Ω_c should be observed. Observed values of Ω_c are also plotted on Figure 8 for comparison, the black dots corresponding to measurements from individual whistler spectrograms and the dashed lines corresponding to the variation of Ω_c during low latitude portions of 7 passes. The pass in Figure 5 is a case where a cutoff frequency of $\Omega_c \simeq 500$ Hz is observed from about 26° to 38° geomagnetic latitude.

V. DISCUSSION OF RESULTS

A comparison of these observed results with the coupling predictions of Jones shows general agreement as to the latitudinal sequence of coupling types. However, several significant discrepancies are evident:

(i) The observed latitudinal transitions of coupling types, as given in Figure 7, are at much lower latitudes (35° to 55° geomagnetic latitude) than predicted by Jones' calculations.

(ii) The latitudinal width of the transition from coupling types C_1 to C_5 is much larger than predicted by Jones' calculations.

(iii) The transition from one coupling type to another is often poorly defined with several different coupling types occurring at the same latitude.

(iv) Partially formed proton whistlers of the type described by Jones (with a cutoff midway between the crossover frequency and the proton gyrofrequency) are rarely observed.

(v) The observed electron whistler cutoff frequencies Ω_c show a large scatter about the curve predicted by Jones.

These disagreements, particularly in regard to the latitudinal transition of coupling types, indicates that sig-

nificant differences must exist between the model used by Jones and the actual whistler propagation in the ionosphere. Some of the essential elements of Jones' calculations which are questionable are discussed below.

A. The Wave Normal Angle. In computing the transition latitudes shown in Figure 3, Jones assumed that the wave normal angle of a whistler is refracted to nearly vertical within the ionosphere. Although this assumption would appear to be reasonable at mid-latitudes where only small latitudinal gradients occur in the ionosphere, no specific experimental data is yet available to support this assumption. On the contrary, if the critical coupling angle θ_c determines the electron whistler cutoff frequency Ω_c, as proposed by Jones, the large scatter of cutoffs shown in Figure 8 indicate that a wide distribution in wave normal angles is possible.

A spread in the wave normal angle distributions of electron whistlers can be expected if the lower boundary of the ionosphere is allowed to have time-dependent density and orientation variations. Upgoing whistlers would then be refracted to angles other than the vertical. Traveling ionospheric disturbances and ionospheric electron concentration irregularities, such as those discussed by Dyson [1967, 1969] and Heisler [1967], might be sources of such variations. A distribution of lightning sources spread out over a large

latitude range below the satellite would also contribute, somewhat, to a distribution of wave normal angles about the vertical.

B. The Critical Coupling Angle. If the wave normal angle is vertical and the transition in coupling types is controlled by the critical coupling angle, as suggested by Figure 2, then the observed transition latitudes imply a typical critical coupling angle of 25 to 30°, rather than 10° or less as computed by GSBS and Jones. Of the ionosphere parameters used to calculate the critical coupling angle, the collision frequency is probably the most uncertain. At high altitudes (~2500 Km) it would be necessary to increase the collision frequencies by a factor of 100 or more above those used by Jones to obtain a critical coupling angle of 25°. Since such large collision frequencies ($\nu \simeq 10$ sec^{-1}) are not evident in the damping of proton whistlers [Gurnett and Brice, 1966] this explanation is not considered possible. These considerations would suggest, therefore, that the critical coupling angle may not be the primary factor controlling the mode coupling of proton whistlers. The observed sharpness of the cutoff frequency Ω_c indicates, instead, that the primary function of the critical coupling angle is to determine which wave normal angles undergo polarization reversal.

C. The Relative Importance of Vertical Gradients and the Critical Coupling Condition. Referring to equation (2), it is seen that the coupling parameter ψ can become large either due to rapid changes in the polarization with respect to height [$\rho' = (1/K)\,\partial\rho/\partial Z$] or due to the polarization approaching the critical coupling condition, $\rho = \pm 1$. Referring to Figure 2, it can be seen that the wave normal angle must be very close (within one or two degrees) of the critical coupling angle for the critical coupling condition to play an important role in making ψ large. Since important coupling effects evidently occur for wave normal angles considerably greater than the critical coupling angle, it appears that vertical gradients in the polarization must be the dominant condition determining the mode coupling of electron and ion whistlers. Further evidence for the importance of ρ' is provided by Figure 2 which shows that, for paths like E - E' which do not even come close to the critical coupling point $\rho = +1$, the polarization changes very rapidly with altitude. For example, along path E - E' the polarization changes from $\rho = 1.9 - i\ 0.8$ to $\rho = 1.8 + i\ 1.2$ in a distance of just 1 Km (from 771.5 to 772.5 Km), which is much less than a typical wavelength ($\sim$10 Km) at that altitude and frequency. Thus, it would appear that detailed predictions of whistler mode coupling cannot be made from Figure 2 simply

from how close the polarization trajectory approaches the critical coupling condition $\rho = +1$ as has been done by Jones. A full understanding of the mode coupling of whistlers in the ionosphere evidently will require complete numerical solutions of the coupled equations.

REFERENCES

Budden, K.G., Radio Waves in the Ionosphere, Cambridge University Press, Cambridge, England, 1961.

Carpenter, D.L., F. Walter, R.E. Barrington, and D.J. McEwen, Alouette 1 and 2 observations of abrupt changes in whistler rate and of VLF noise variations at the plasma pause -- A satellite-ground study, J. Geophys. Res., 73, 2929, 1968.

Dyson, P.L., Topside refractive irregularities and traveling ionospheric disturbances, Australian J. Phys., 20, 467, 1967.

Dyson, P.L., Direct measurements of the size and amplitude of irregularities in the topside ionosphere, J. Geophys. Res., 74, 6291, 1969.

Gurnett, D.A., and N.M. Brice, Ion temperature in the ionosphere obtained from cyclotron damping of proton whistlers, J. Geophys. Res., 71, 3639, 1966.

Gurnett, D.A., and B.J. O'Brien, High latitude geophysical studies with satellite Injun 3, 5. Very-low-frequency electromagnetic radiation, J. Geophys. Res., 69, 65, 1964.

Gurnett, D.A., S.D. Shawhan, N.M. Brice, and R.L. Smith, Ion cyclotron whistlers, J. Geophys. Res., 70, 1665, 1965.

Gurnett, D.A., G. William Pfeiffer, Roger R. Anderson, Stephen R. Mosier, and David P. Cauffman, Initial observations of VLF electric and magnetic fields with the Injun 5 satellite, J. Geophys. Res., 74, 4631, 1969.

Heisler, L.H. Traveling ionospheric disturbances, Space Res., 7, 55, 1967.

Heyborne, R.L., R.L. Smith, and R.A. Helliwell, Latitudinal cutoff of VLF signals in the ionosphere, J. Geophys. Res., 74, 2393, 1969.

Jones, D., The Theory of the effect of collisions on ion cyclotron whistlers, paper presented at the NATO Advanced Study Institute on Plasma Waves in Space and in the Laboratory, Røros, Norway, April 17-26, 1968.

Jones, D., The effect of the latitudinal variation of the terrestrial magnetic field strength on ion cyclotron whistlers, J. Atmosph. Terr. Phys., 31, 971, 1969.

Smith, R.L., N.M. Brice, J. Katsufrakis, D.A. Gurnett, S.D. Shawhan, J.S. Belrose, R.E. Barrington, An ion gyrofrequency phenomenon observed in satellites, Nature, 204, (4955), 274, Oct. 17, 1964.

Smith, R.L., and Neil Brice, Propagation in multicomponent plasmas, J. Geophys. Res., 69, 5029, 1964.

Stix, T.H., The Theory of Plasma Waves, McGraw-Hill Book Company, New York, 1962.

Taylor, Jr., H.A., H.C. Brinton, D.L. Carpenter, F.M. Bonner, and R.L. Heyborne, Ion depletion in the high-latitude exosphere; simultaneous OGO 2 observations of the light ion trough and the VLF cutoff, J. Geophys. Res., 74, 3517, 1969.

FIGURE CAPTIONS

Figure 1 Various critical frequencies vs. altitude for a typical model ionosphere.

Figure 2 Polarization path in the complex ρ plane vs. altitude [From Jones, 1968].

Figure 3 Regions of fully-formed, partially-formed, and no-proton whistlers from Jones [1968].

Figure 4 Classification of coupling types from frequency-time spectrograms of proton whistlers.

Figure 5 Spectrograms of proton whistlers showing a clear transition of coupling types.

Figure 6 Spectrograms of proton whistlers showing a mixture of coupling types with no clear

Figure 7 Occurrence plot of coupling types (A - A') compared with Jones' plot.

Figure 8 Electron whistler cutoff frequency Ω_c vs. latitude and comparison with Jones' calculated dependence of Ω_c on latitude.

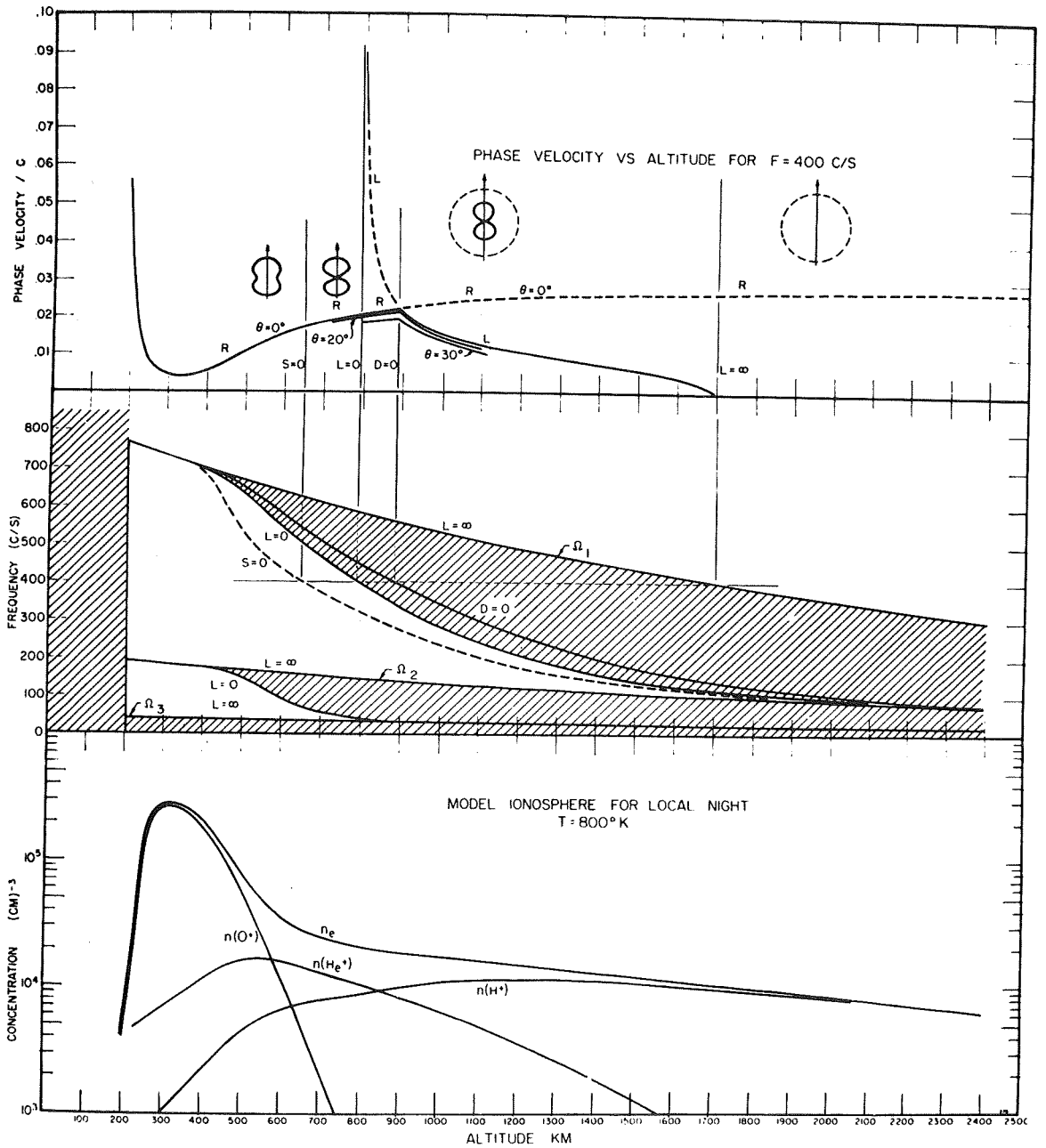
PHASE VELOCITY VS ALTITUDE FOR F = 400 C/S
PHASE VELOCITY / c
FREQUENCY (C/S)
MODEL IONOSPHERE FOR LOCAL NIGHT
T = 800° K
CONCENTRATION (CM)-3
ALTITUDE KM
θ=0°
θ=20°
θ=30°
S=0
L=0
D=0
L=∞
Ω1
Ω2
Ω3
n(O+)
ne
n(He+)
n(H+)

Figure 1

A-G69-177

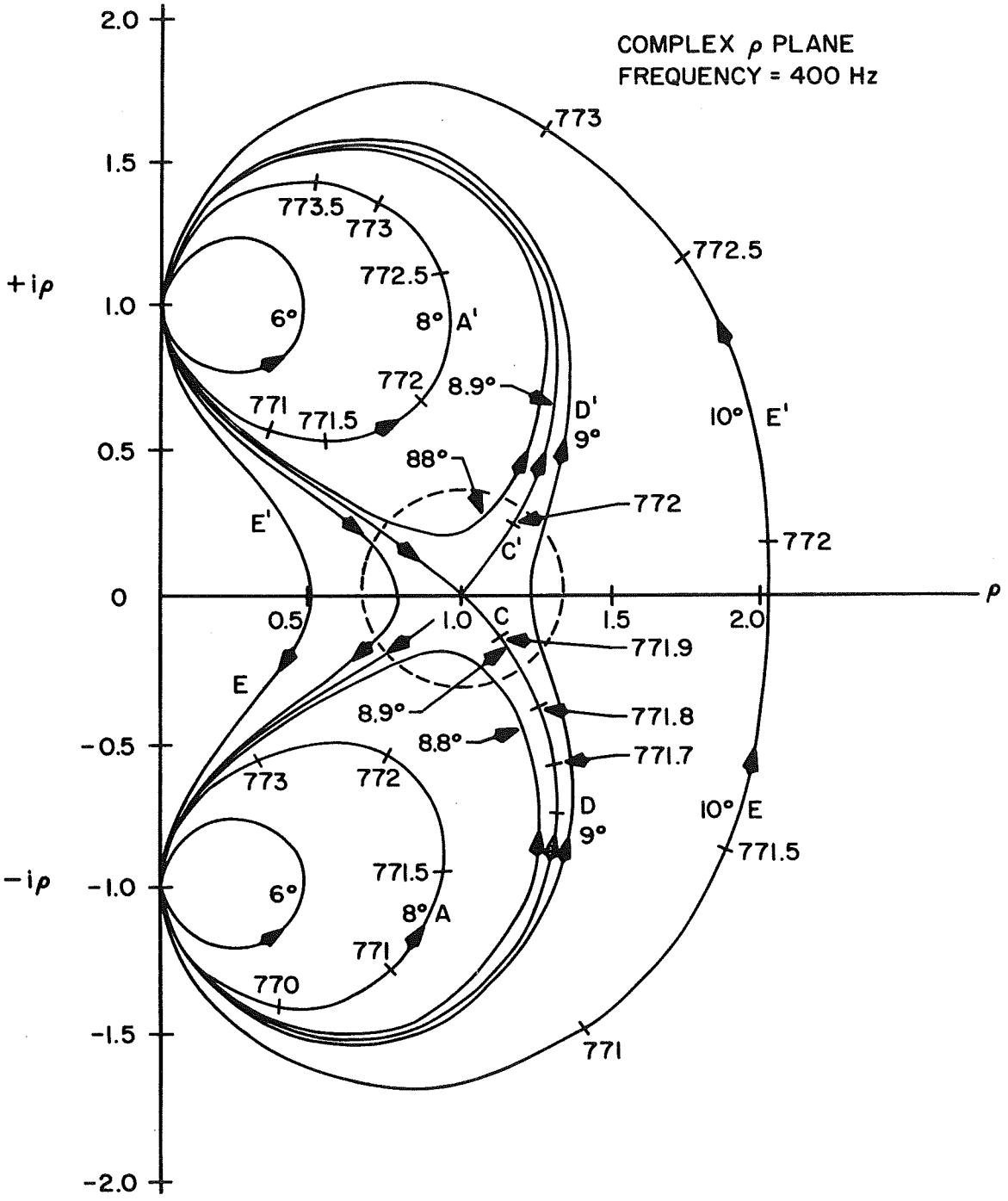

Figure 2

A-670-39

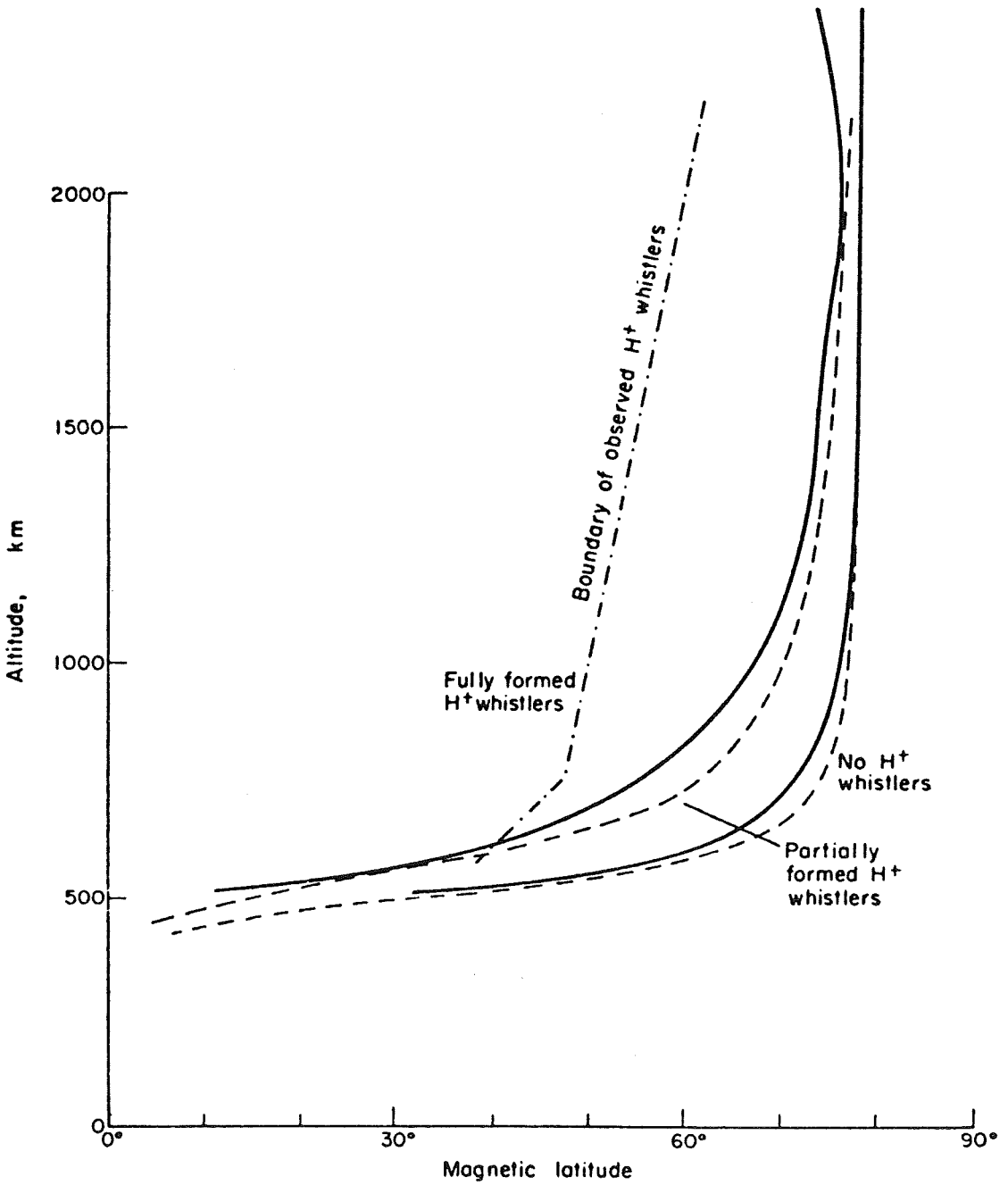

Figure 3

C-G70-130-2

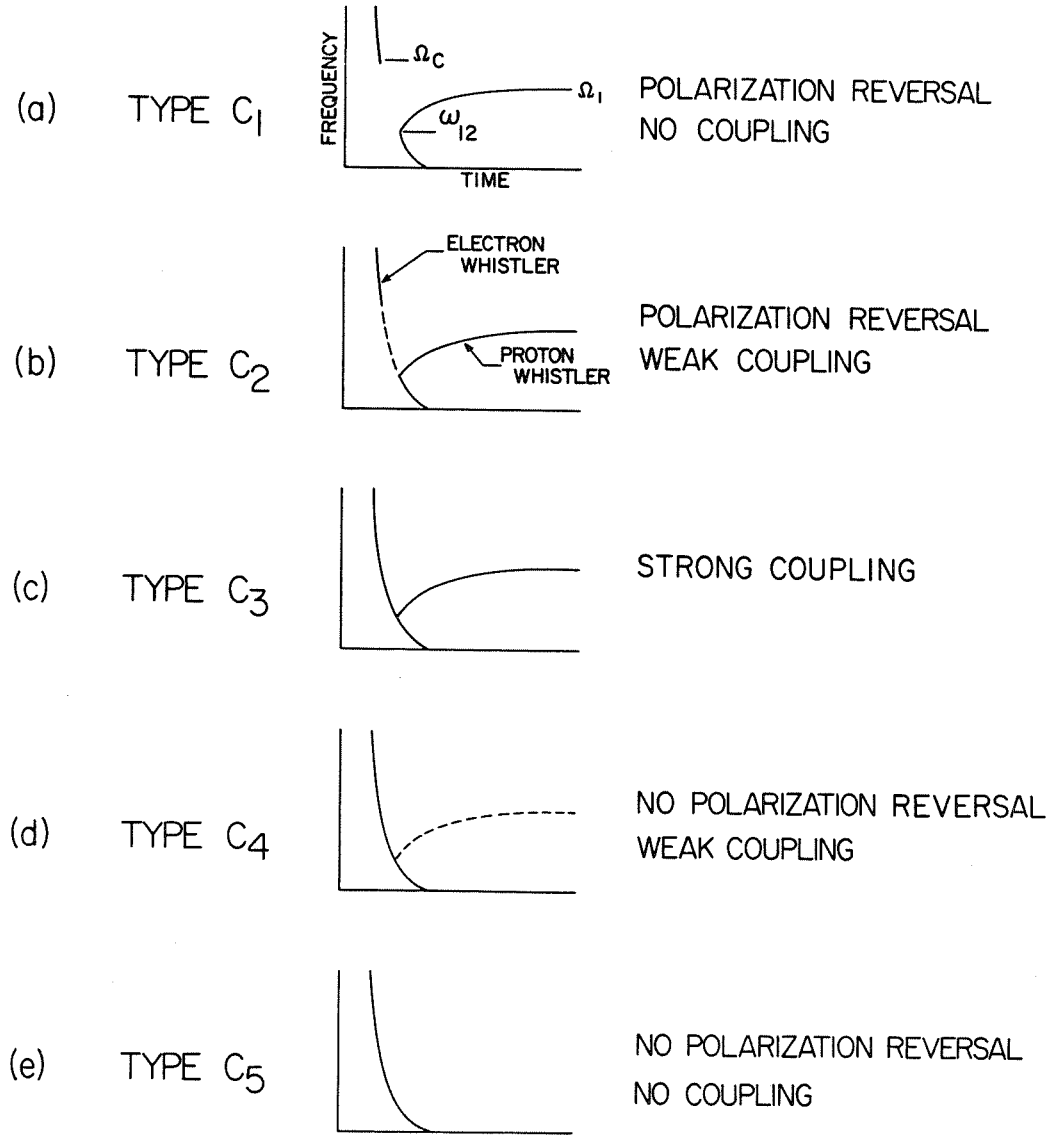

Figure 4

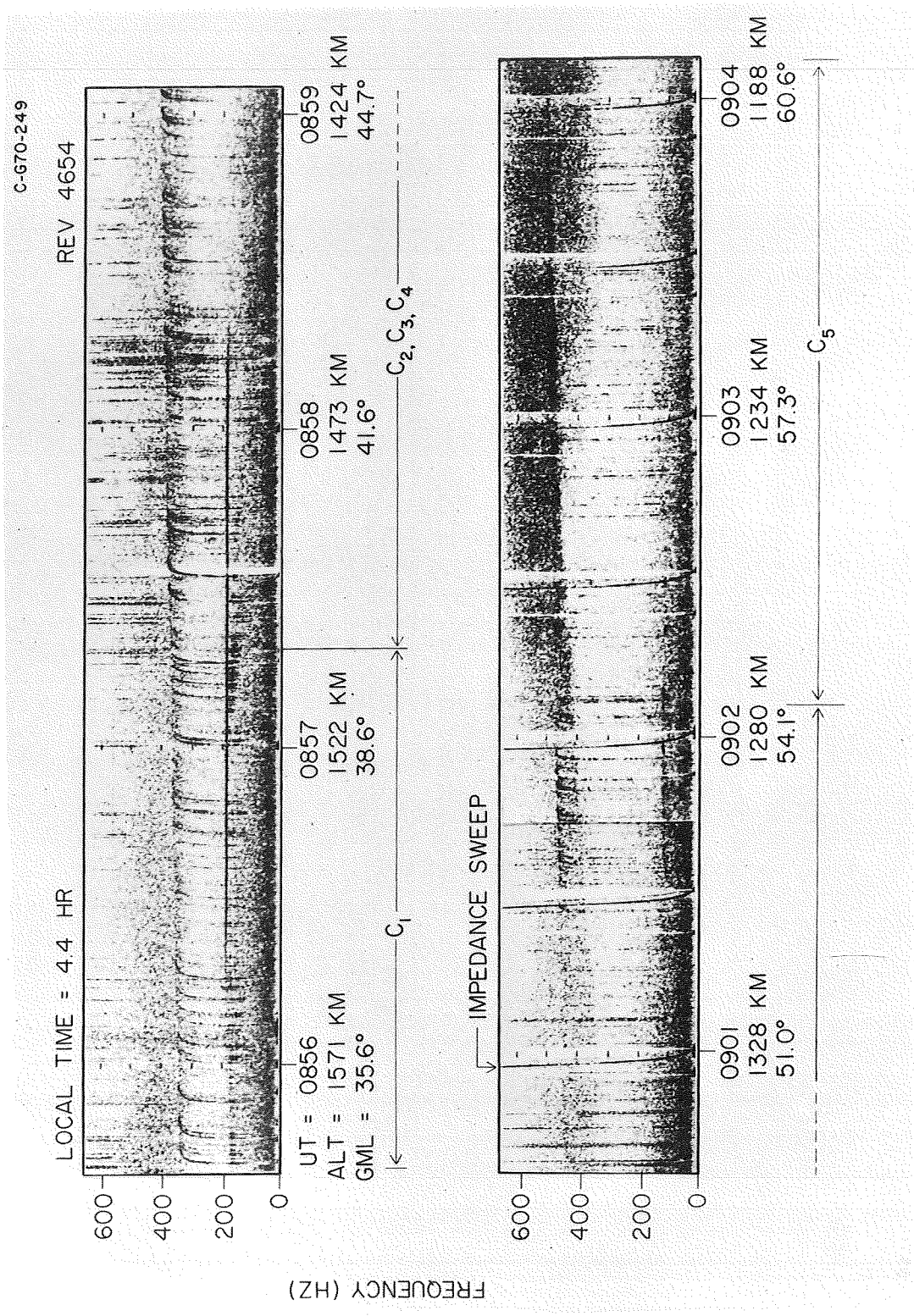
C-670-249
REV 4654
LOCAL TIME = 4.4 HR
UT = 0856
ALT = 1571 KM
GML = 35.6°
0857
1522 KM
38.6°
0858
1473 KM
41.6°
0859
1424 KM
44.7°
C1
C2, C3, C4
IMPEDANCE SWEEP
0901
1328 KM
51.0°
0902
1280 KM
54.1°
0903
1234 KM
57.3°
0904
1188 KM
60.6°
C5
600
400
200
0
FREQUENCY (HZ)

Figure 5

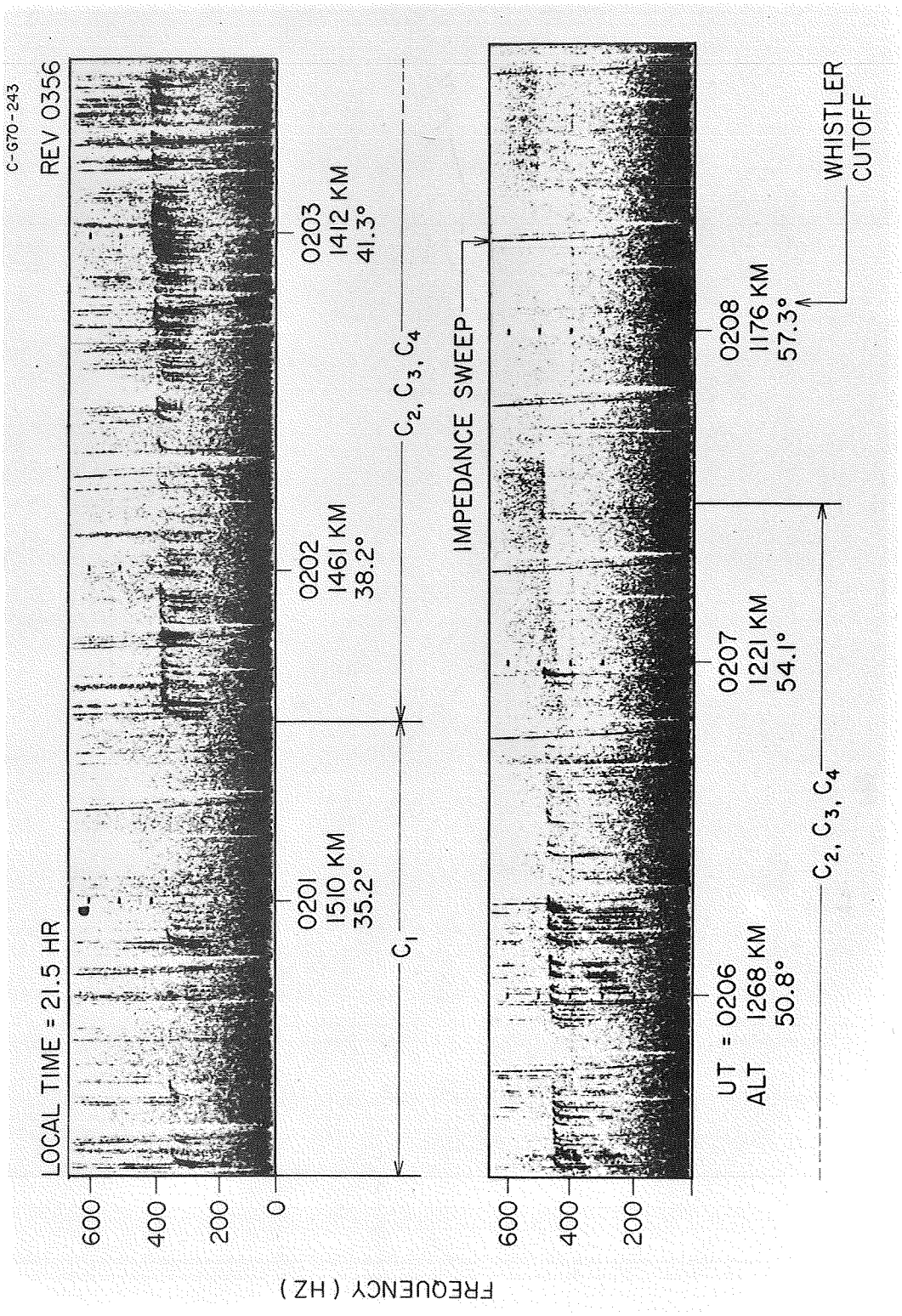
C-G70-243
REV 0356
LOCAL TIME = 21.5 HR
0201
1510 KM
35.2°
0202
1461 KM
38.2°
0203
1412 KM
41.3°
C1
C2, C3, C4
IMPEDANCE SWEEP
UT = 0206
ALT 1268 KM
50.8°
0207
1221 KM
54.1°
0208
1176 KM
57.3°
WHISTLER
CUTOFF
C2, C3, C4
600
400
200
0
600
400
200
FREQUENCY (HZ)

Figure 6

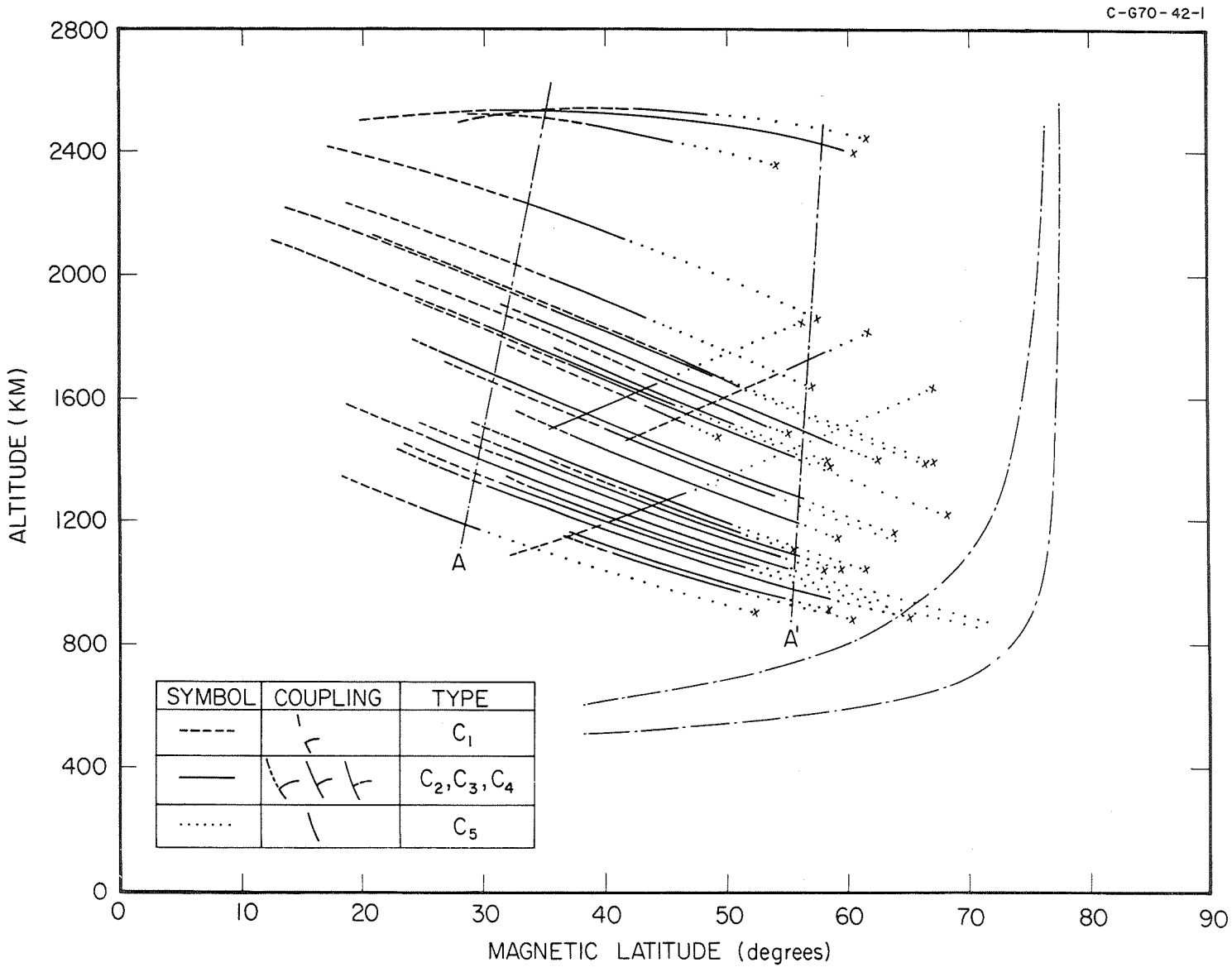
C-G70-42-I
2800
2400
2000
1600
1200
800
400
0
ALTITUDE (KM)
0
10
20
30
40
50
60
70
80
90
MAGNETIC LATITUDE (degrees)
A
A'
SYMBOL
COUPLING
TYPE
C1
C2,C3,C4
C5

Figure 7

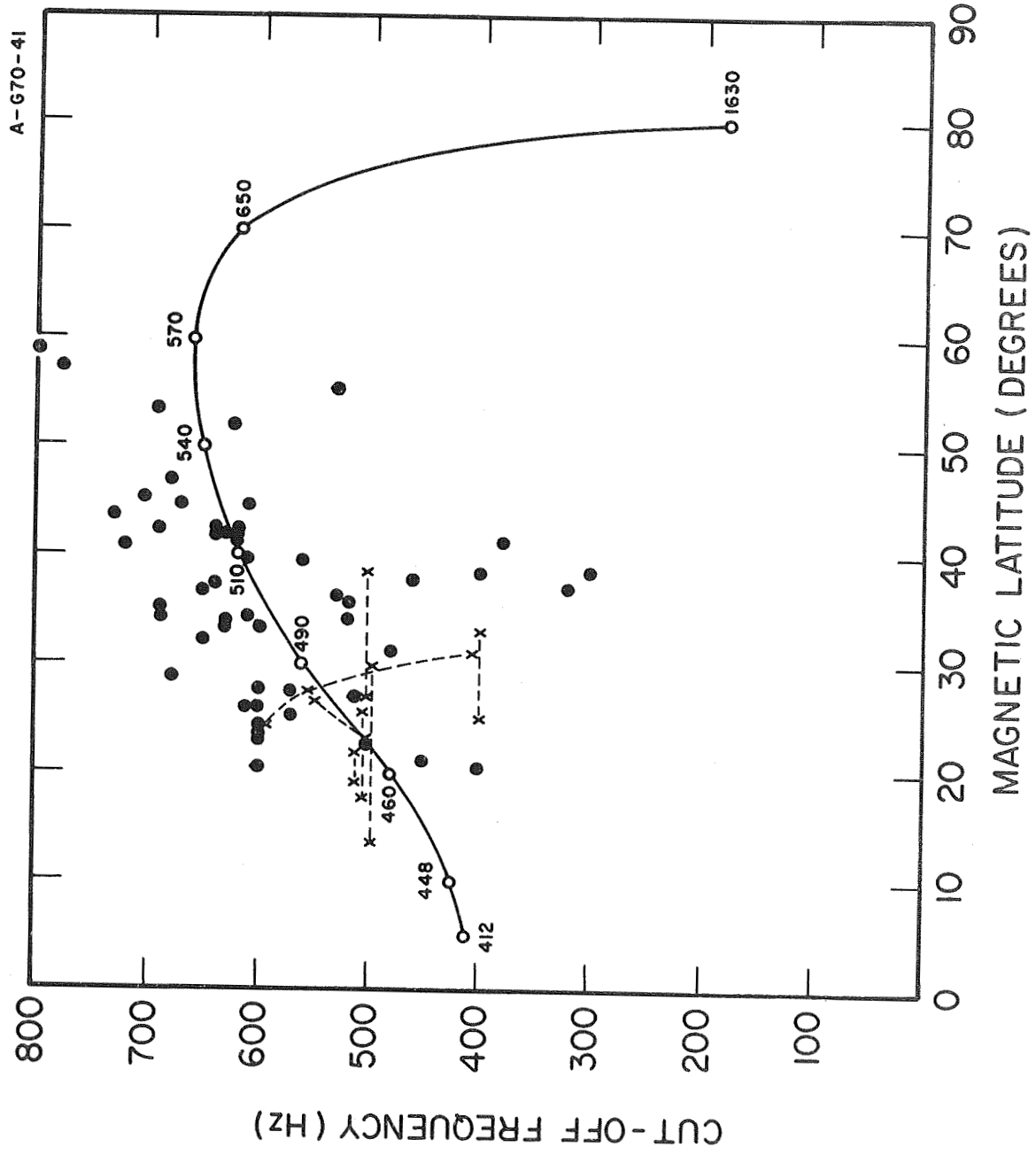
A-G70-41
1630
650
570
540
510
490
460
448
412
800
700
600
500
400
300
200
100
0
10
20
30
40
50
60
70
80
90
CUT-OFF FREQUENCY (Hz)
MAGNETIC LATITUDE (DEGREES)

Figure 8